JOC The Journal of Organic Chemistry

Article

pubs.acs.org/joc

The Conformations of Cyclooctene: Consequences for Epoxidation Chemistry

Ulrich Neuenschwander and Ive Hermans*

Department of Chemistry and Applied Bio-Sciences, ETH Zurich, Wolfgang-Pauli-Str. 10, 8093 Zurich, Switzerland

Supporting Information

ABSTRACT: The conformational space of cyclooctene has been explored computationally in order to rationalize its high epoxidation selectivity. Four different conformations were identified. Each conformation is chiral and has two enantiomeric forms. The degeneracy is further increased by a ring-inversion process, yielding a total of 16 conformers. The potential energy surface for the interconversion of these conformers was characterized via intrinsic reaction coordinate analyses. Furthermore, an evaluation of the micro-canonical partition functions allowed for a quantification of the entropy contributions and hence the calculation of the equilibrium composition at different temperatures. The results strongly suggest that the high epoxidation selectivity, typically observed for cyclooctene, is related to a poor $\sigma_{C-\alpha H}-\pi_{C=C}$ orbital overlap in the predominant conformation, disfavoring αH-abstraction by radical species and thus allylic byproduct formation via undesired homolytic side-reactions.

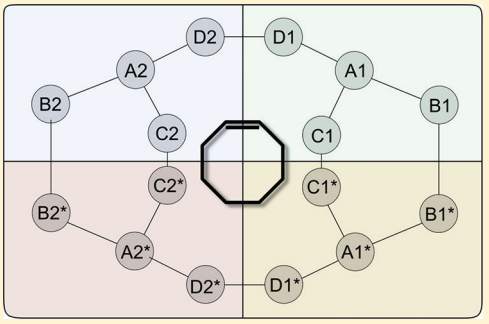

INTRODUCTION

The epoxidation of cyclooctene is a favorable oxidative transformation and the subject of many studies.[1] In general, a low amount of undesired allylic byproducts, stemming from homolytic side-reactions, is observed for this particular substrate. Even under (radical) autoxidation conditions, using O_2 as the oxidant, cyclooctene yields a higher epoxide selectivity than other cyclic alkenes.[2] The reason(s) for this peculiar behavior of cyclooctene is not immediately evident.

The commercially available stereoisomer is (*Z*)-cyclooctene. For (*E*)-cyclooctene, which is the smallest (*E*)-cycloalkene that has been isolated, three ground state conformations have been identified by Olson[3] and Bach.[4] Because of its high ring-strain, particular reactivities can be achieved.[5] Yet, the energy of the (*E*) form is significantly higher than that of the (*Z*) form, and dedicated synthetic routes are required for its synthesis. Therefore, in this paper cyclooctene refers to (*Z*)-cyclooctene, unless specifically mentioned.

Surprisingly, the conformations of cyclooctene have not yet been verified in detail. The only available data are based on rough estimates using group increment[6] or force field[7] approaches, concluding that cyclooctene has a nondescript, flexible conformation. In this contribution, we aim for a full structural analysis of cyclooctene and, consequently, a better understanding of its peculiar reactivity.

METHODS

The different cyclooctene conformations were optimized at the B3LYP-DFT/6-31G(d,p) level of theory.[8] The reported relative energies of the stationary points include the contribution of zero-point energy (ZPE; B3LYP/6-31G(d,p)-level), unless explicitly mentioned. The relative energies of the different conformations were further refined by single point-calculations at the B3LYP/6-311++G(df,pd), CCSD(T)/6-31G(d,p), and G2M[9] levels; G2M refers, in this paper, to the energy computed as E[CCSD(T)/6-31G(d,p)//B3LYP/6-31G(d,p)] + {E[MP2/6-311++G(df,pd)//B3LYP/6-31G(d,p)] − E[MP2/6-31G-(d,p)//B3LYP/6-31G(d,p)]} + ZPE[B3LYP/6-31G(d,p)]. The transition states connecting the different conformations were subjected to intrinsic reaction coordinate (IRC) analyses (the zero point of these IRCs was chosen arbitrarily). All calculations were performed with Gaussian 09.[10]

RESULTS AND DISCUSSION

Identifying the Basic Conformations. Four different energy minima were identified on the potential energy surface, denoted below as **A**, **B**, **C**, and **D**. These minima correspond to four different conformations of (*Z*)-cyclooctene. The most stable conformation **A** has a structure with four carbon atoms in plane (C−C=C−C) and four carbon atoms above that plane. Conformation **C** is similar, but with different dihedral angles. Conformations **B** and **D** represent situations with five carbon atoms in plane (C−C=C−C−C). Three orthogonal projections of each conformation are provided in Figure 1. The Cartesian coordinates can be found in the Supporting Information.

The interconversion of these four conformations occurs via internal C−C rotations, starting from the central conformation **A**, connecting to **B**, **C**, and **D**. The potential energy surface (PES) of these three conformational changes is given in Figure 2, from which the relative, energetic order of the conformations can be identified as **A** < **B** < **D** < **C**.

The ZPE-corrected single-point values of the four conformations' relative energies are given in Table 1. It is interesting to notice that the DFT//DFT, the CCSD(T)//DFT, and the G2M//DFT results all agree within 1 kcal mol^{-1}.

Received: October 20, 2011
Published: November 13, 2011

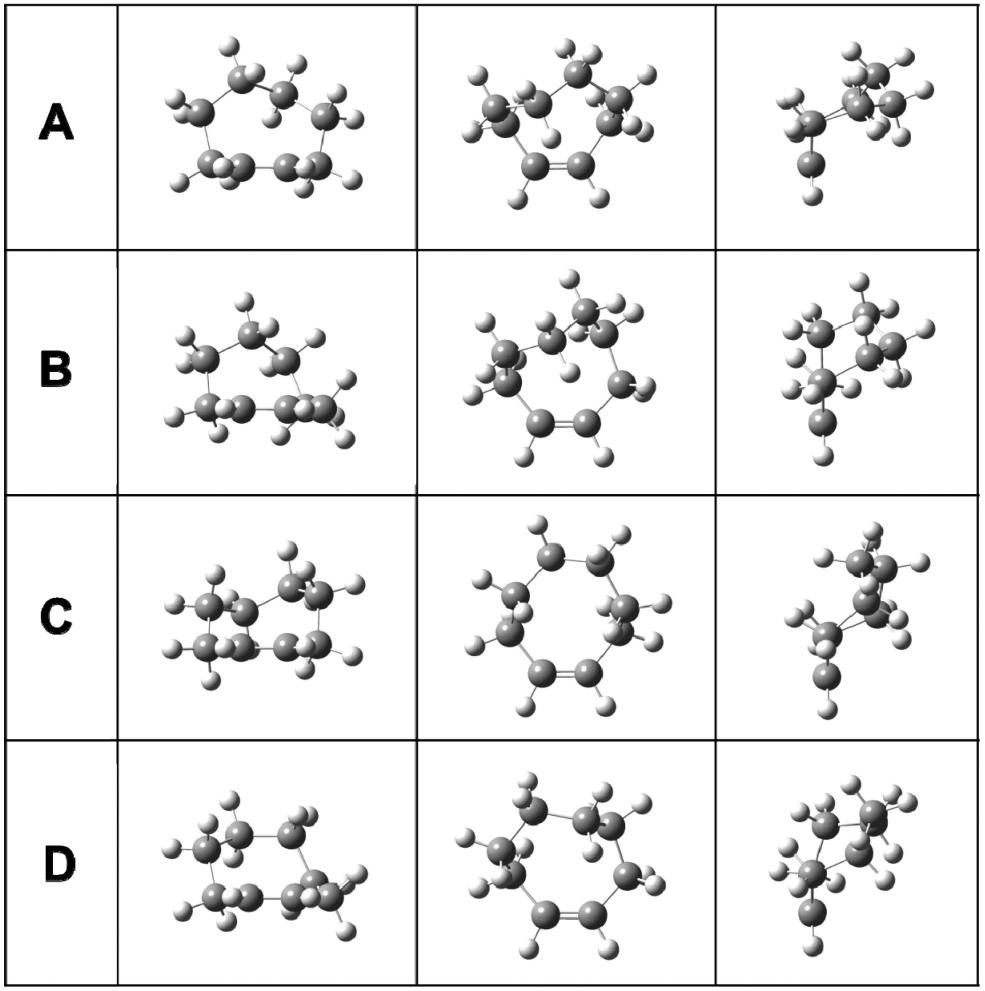

Figure 1. Orthogonal projections of the conformations **A**–**D**.

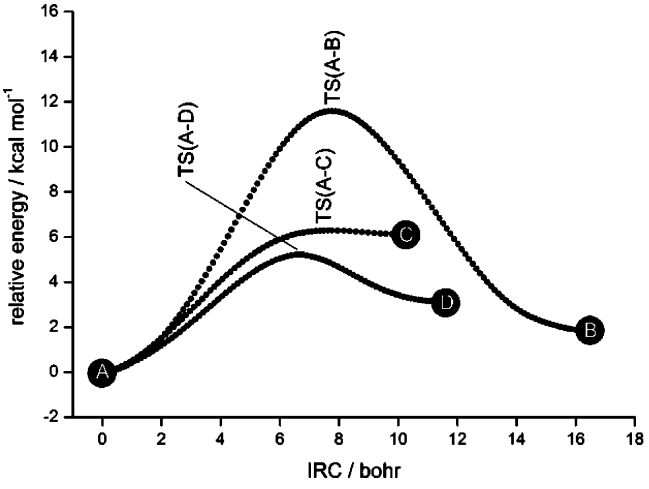

Figure 2. PES of the internal C–C rotations in conformation **A** that lead to the conformations **B**, **C**, and **D**. B3LYP/6-31G(d,p) level of theory without ZPE-corrections.

This observation does not only justify the use of DFT for the geometry optimization, it also suggest a small influence of the basis set on the CCSD(T) calculation for this particular system, as the MP2 basis set extrapolation in the G2M method barely changes the CCSD(T) results. In order to calculate the equilibrium population of the conformations, the partition functions

Table 1. Relative Energies of the Four Identified Cyclooctene Conformations, as well as Their Partition Functions and Population Contributions at 298 K

conformer	DFT[a] (kcal mol^{-1})	CCSD(T)[b] (kcal mol^{-1})	G2M[c] (kcal mol^{-1})	Q_{tot} (m^{-3})	pop.[d] (%)
A	0.0	0.0	0.0	4.49×10^{40}	96.0
B	2.0	2.1	2.1	6.73×10^{40}	3.8
C	5.7	6.5	6.4	2.52×10^{41}	0.01
D	3.0	4.0	4.0	8.71×10^{40}	0.23

[a]B3LYP/6-311++G(df,pd)//B3LYP/6-31G(d,p) level of theory. [b]CCSD(T)/6-31G(d,p)//B3LYP/6-31G(d,p) level of theory. [c]G2M level of theory (see Methods). [d]Values are based on the G2M relative energies.

Q_{tot} were evaluated according to eq 1. Q_{trans} refers to the translational partition function (three-dimensional particle-in-a-box model), Q_{rot} is the rotational partition function (rigid rotor model), and Q_{vib} is the vibrational partition function (harmonic oscillator model).[11] With that in mind, the equilibrium constants for the isomerization between two arbitrary conformations i and j can be computed using van't Hoff eq 2.

$$Q_{tot} = Q_{trans} \times Q_{rot} \times Q_{vib} \quad (1)$$

$$K_{i \to j} = \frac{[j]}{[i]} = \frac{Q_j}{Q_i} \times \exp\left(- \frac{E_j - E_i}{RT} \right) \quad (2)$$

dx.doi.org/10.1021/jo202176j | J. Org. Chem. 2011, 76, 10236–10240

According to these calculations, the population of conformation **A** is 96% at room temperature (see Table 1), with the remainder primarily consisting of **B** and **D**. An analogous analysis leads to the conformation population at different temperatures. The resulting temperature-dependence of the equilibrium composition is plotted in Figure 3.

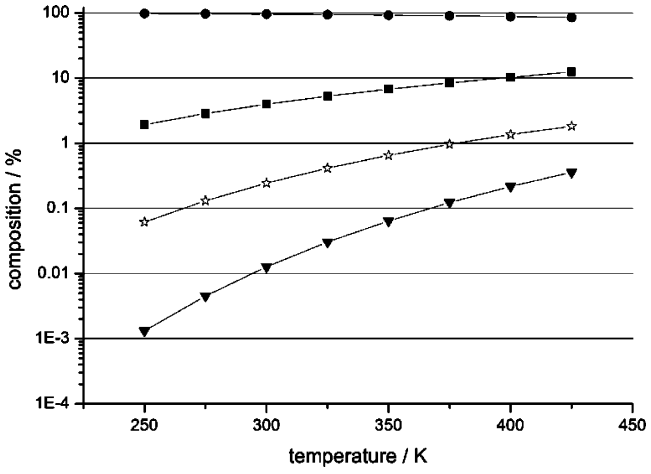

Figure 3. Equilibrium composition at different temperatures. Conformations **A** (●), **B** (■), **C** (▼), and **D** (☆).

Stereochemistry. It is noteworthy that none of the conformations **A**–**D** feature an internal rotation-reflection axis (S_n with $n \in \mathbb{N}_0$), implying that all of them are chiral. Since the systematic (*R*/*S*) nomenclature for planar chirality is not applicable to compounds of such highly symmetric constitution,[12] we define the enantiomers of **A**, **B**, **C**, and **D** in an arbitrary way as **A***, **B***, **C***, and **D***, respectively.

Racemisation processes (e.g., the inversion of **A** to **A***) must be accomplished with achiral transition states. In the case of cyclooctene, they have C_s symmetry (the reflection plane intersecting the C=C bond orthogonally). Two versions are possible: The first possibility is the **B**–**B*** transition, featuring a perfect boat conformation, and the second possibility is the **C**–**C*** transition, featuring a perfect chair conformation (Figure 4).

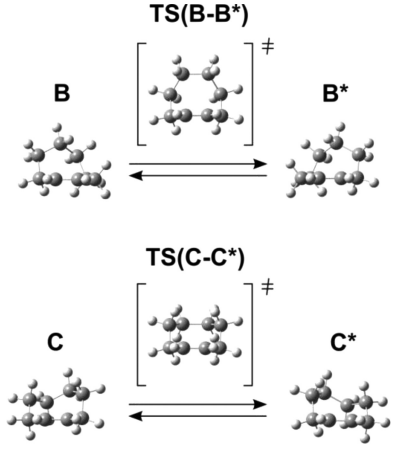

Figure 4. Boat and chair conformations, corresponding to the transition structures TS(**B**–**B***) and TS(**C**–**C***).

As a conclusion, the highly symmetric boat and chair forms are actually transition states, not stable conformations. This is in contrast to the earlier work of Favini and Allinger.[6,7] The potential energy surface is such that racemization of **A** to **A*** (and vice versa) occurs preferentially via racemization of **C** to **C*** (Figure 5). As a second pathway, the route via **B** and **B*** is possible, but the activation energy is significantly higher.

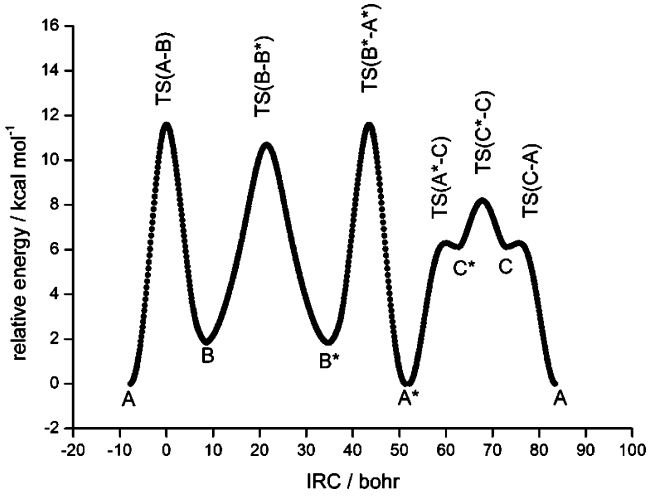

Figure 5. PES of the racemization of the **A**, **B**, and **C** conformers. B3LYP/6-31G(d,p) level of theory without ZPE-corrections.

Full Conformational Space. On the other hand, an enantioretentive ring-inversion of a similar type to the chair–chair inversion exhibited by cyclohexane is also possible. Indeed, by ring-inversion of a **D** conformer, the four carbon atoms above the plane can migrate below the plane, forming another **D** conformer. Although this second **D** conformer is stereochemically identical to the first one, it constitutes a new point in the conformational space (just as cyclohexane has two identical chair conformers). Therefore, we denote these two conformers as **D1** and **D2**, the numbers indicating the relative position with respect to the olefin's sp^2 plane. The transition state that connects **D1** with **D2** was shown to possess "twist" geometry (Figure 6). In agreement with the conservation of

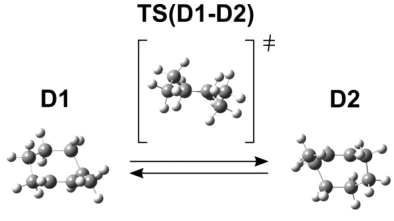

Figure 6. The **D1** and **D2** conformers, with a "twist" transition state connecting them.

chirality in that process, this "twist" transition structure is chiral and has C_2 symmetry.

In a subsequent conformational change, the conformer **D2** can convert back to an **A**-equivalent conformer **A2**, in the same way as shown in Figure 1. In summary, for the ring-inversion of the most stable conformer **A1** into its analogous form **A2**, two intermediates **D1** and **D2** are traversed (see Figure 7).

dx.doi.org/10.1021/jo202176j | J. Org. Chem. 2011, 76, 10236–10240

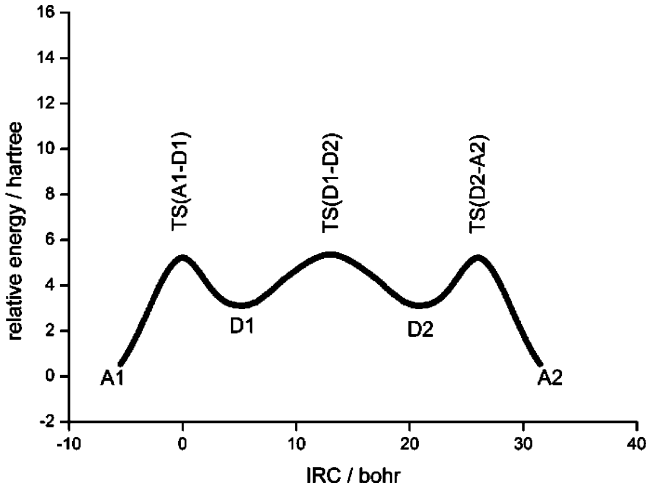

Figure 7. PES of the ring-inversion. The decisive "twist" TS connects **D1** and **D2**. B3LYP/6-31G(d,p) level of theory without ZPE-corrections.

With all these processes shown so far, the entire conformational space can be covered. Note that all the energetics that apply to the relation among the **A**, **B**, **C**, and **D** conformations are congruent with the energetics that apply to the relation among their enantiomeric counterparts **A***, **B***, **C***, and **D***.[13] As an overview, Figure 8 sketches the conformational space of cyclooctene. The

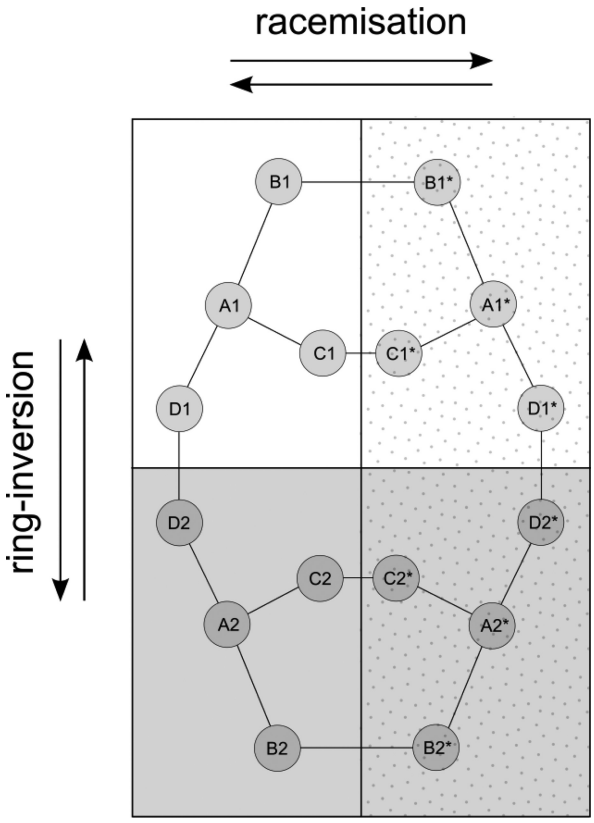

Figure 8. Full conformational space of cyclooctene. Stars denote enantiomers. The numbers 1 and 2 refer to above or below the olefin's sp^2 plane, respectively.

four basic conformations are each 4-fold degenerate (thermal population is given in Figure 3), yielding a total of 16 conformers.

Epoxidation vs Allylic Oxidation. It is generally accepted that allylic byproducts arise under epoxidation conditions upon αH-abstraction by radicals,[1e] generated via undesirable homolytic side-reaction. It is interesting, therefore, that the allylic H-atoms in the **A** conformation are almost in the olefin's sp^2 plane; i.e., the σ_{C-H} orbital is close to orthogonal to the $\pi_{C=C}$ orbital. Therefore, the overlap between those two orbitals is poor. However, to facilitate efficient allylic H-abstraction, the overlap should be as strong as possible, such that the transition state can benefit from partial allyl radical character.[14] Figure 9 illustrates this situation.

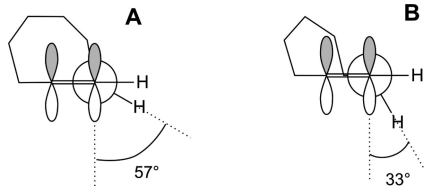

Figure 9. Newman projection of conformations **A** and **B**. In conformation **A**, the allylic H atom is pointing away from the $\pi_{C=C}$ orbital. In conformation **B**, the H atom is more parallel to $\pi_{C=C}$.

As a consequence, the abstraction of allylic H-atoms is not very favorable in the most stable cyclooctene conformation. For instance, the calculated H-abstraction activation barrier with the peroxyl radical $CH_3OO^\bullet$ is 13.1 kcal mol^{-1}; the barrier for addition of the $CH_3OO^\bullet$ radical to the C=C bond is only 11.2 kcal mol^{-1} (this addition step is rapidly followed by a unimolecular Twigg rearrangement[15] to epoxide plus $CH_3O^\bullet$; see Figure 10). In agreement with the relative order of the ground state stabilities and the geometric considerations made in Figure 9, the high-lying H-abstraction TS (leading to allylic byproduct) is **B**-like, whereas the low-lying addition TS (leading to epoxide) is **A**-like. As a consequence, if by some unwanted side-reactions peroxyl radicals are occurring in a particular (catalytic) epoxidation system, they preferentially add to the C=C bond, forming cyclooctene oxide rather than allylic byproduct (Figure 10). Thus, a high chemoselectivity is maintained, even if some radical side-reactions are occurring.

By calculating the same competition between allylic H-abstraction and addition to the C=C bond (leading to epoxidation) for the substrates cycloheptene, cyclohexene, and cyclopentene, the peculiar reactivity of cyclooctene can be illustrated persuasively (Figure 11). Although the addition barriers for all these substrates are roughly the same (ca. 11.5 kcal mol^{-1}), the abstraction barriers are consistently lower by ca. 3 kcal mol^{-1}, as compared to cyclooctene. Therefore, the aptitude for allylic oxidation is smallest for cyclooctene, in agreement with the experimental observations.[2]

■ CONCLUSIONS

Four conformations of (*Z*)-cyclooctene, **A**–**D**, have been characterized. Because of their chirality, four enantiomeric counterparts are possible. The racemization occurs via two pathways: **B**–**B*** and **C**–**C***. With ring-inversion, starting from the **D** conformation, a stereoidentical conformer can be attained, labeled **D2**. Consequently, there are four conformers per conformation accessible, i.e., 16 conformers in total. The high epoxidation tendency of cyclooctene can be rationalized with the transition state for radical epoxidation having character of the lowest conformation, i.e., **A**, and the transition state for

dx.doi.org/10.1021/jo202176j | J. Org. Chem. 2011, 76, 10236–10240

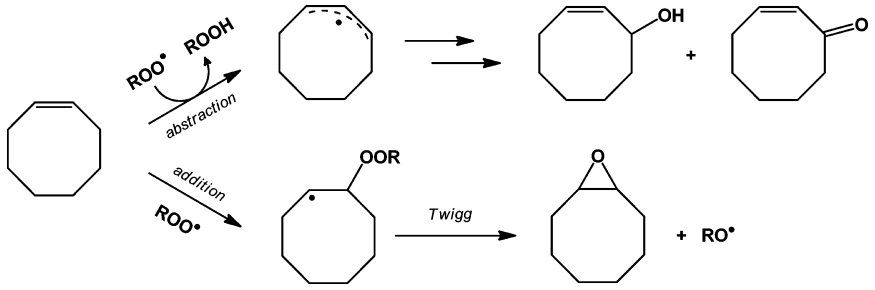

Figure 10. Reactivity of cyclooctene with peroxyl radicals. Above: Allylic H-abstraction, leading to allylic side-products. Below: Addition to the C═C bond and subsequent Twigg rearrangement to epoxide.

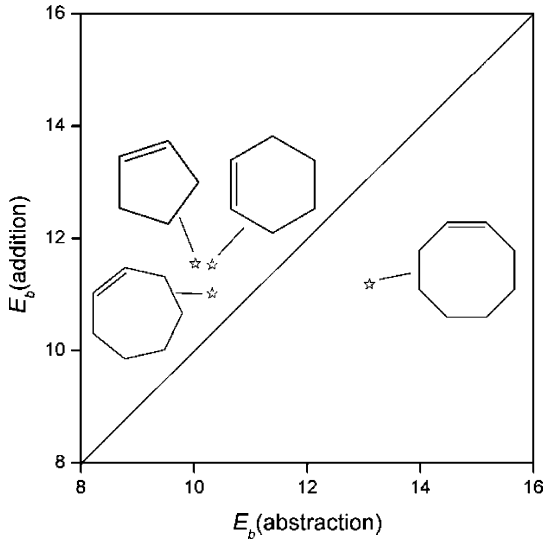

Figure 11. Addition barrier vs abstraction barrier for various substrates (B3LYP/6-311++G(df,pd)//B3LYP/6-31G(d,p) level of theory). The diagonal line indicates equal barriers for abstraction and addition reactions.

allylic oxidation having character of a conformation of higher energy, i.e., **B**. For this particular substrate, allylic H-abstraction by radicals is disfavored, explaining the high epoxide selectivity that is typically associated with cyclooctene.

■ ASSOCIATED CONTENT

Ⓢ Supporting Information

Cartesian coordinates of the optimized conformations and transition states. This material is available free of charge via the Internet at http://pubs.acs.org.

■ AUTHOR INFORMATION

Corresponding Author

*E-mail: hermans@chem.ethz.ch.

■ ACKNOWLEDGMENTS

The authors acknowledge the financial support from the Swiss National Science Foundation (SNF) and ETH Zurich.

■ REFERENCES

(1) (a) Jia, M.; Seifert, A.; Thiel, W. R. *Chem. Mater.* **2003**, *15*, 2174. (b) Kamata, K.; Yonehara, K.; Sumida, Y.; Yamaguchi, K.; Hikichi, S.; Mizuno, N. *Science* **2003**, *300*, 964. (c) Stephenson, N. A.; Bell, A. T. *J. Am. Chem. Soc.* **2005**, *127*, 8635. (d) Adolfsson, H.; Copéret, C.; Chiang, J. P.; Yudin, A. K. *J. Org. Chem.* **2000**, *65*, 8651. (e) Oyama, S. T. *Mechanisms in Homogeneous and Heterogeneous Epoxidation Catalysis*; Elsevier: Amsterdam, 2008.

(2) van Sickle, D. E.; Mayo, F. R.; Arluck, R. M. *J. Am. Chem. Soc.* **1965**, *87*, 8635.

(3) Olson, L. P. *Internet J. Chem.* **1999**, 2.

(4) Bach, R. D. *J. Am. Chem. Soc.* **2009**, *131*, 5233.

(5) (a) Taylor, M. T.; Blackman, M. L.; Dmitrenko, O.; Fox, J. M. *J. Am. Chem. Soc.* **2011**, *133*, 9646. (b) Devaraj, N. K.; Upadhyay, R.; Haun, J. B.; Hilderbrand, S. A.; Weissleder, R. *Angew. Chem.* **2009**, *121*, 7147.

(6) Favini, G.; Buemi, G.; Raimondi, M. *J. Mol. Struct.* **1968**, *2*, 137.

(7) Allinger, N. L.; Sprague, J. T. *J. Am. Chem. Soc.* **1972**, *94*, 5734.

(8) (a) Becke, A. D. *J. Chem. Phys.* **1992**, *96*, 2115. (b) Becke, A. D. *J. Chem. Phys.* **1992**, *97*, 9173. (c) Becke, A. D. *J. Chem. Phys.* **1993**, *98*, 5648. (d) Lee, C.; Yang, W.; Parr, R. G. *Phys. Rev. B: Condens. Matter Mater. Phys.* **1988**, *37*, 785.

(9) Mebel, A. M.; Morokuma, K.; Lin, M. C. *J. Chem. Phys.* **1995**, *103*, 7414.

(10) Frisch, M. J.; Trucks, G. W.; Schlegel, H. B.; Scuseria, G. E.; Robb, M. A.; Cheeseman, J. R.; Scalmani, G.; Barone, V.; Mennucci, B.; Petersson, G. A.; Nakatsuji, H.; Caricato, M.; Li, X.; Hratchian, H. P.; Izmaylov, A. F.; Bloino, J.; Zheng, G.; Sonnenberg, J. L.; Hada, M.; Ehara, M.; Toyota, K.; Fukuda, R.; Hasegawa, J.; Ishida, M.; Nakajima, T.; Honda, Y.; Kitao, O.; Nakai, H.; Vreven, T.; Montgomery, J. A., Jr..; Peralta, J. E.; Ogliaro, F.; Bearpark, M.; Heyd, J. J.; Brothers, E.; Kudin, K. N.; Staroverov, V. N.; Kobayashi, R.; Normand, J.; Raghavachari, K.; Rendell, A.; Burant, J. C.; Iyengar, S. S.; Tomasi, J.; Cossi, M.; Rega, N.; Millam, N. J.; Klene, M.; Knox, J. E.; Cross, J. B.; Bakken, V.; Adamo, C.; Jaramillo, J.; Gomperts, R.; Stratmann, R. E.; Yazyev, O.; Austin, A. J.; Cammi, R.; Pomelli, C.; Ochterski, J. W.; Martin, R. L.; Morokuma, K.; Zakrzewski, V. G.; Voth, G. A.; Salvador, P.; Dannenberg, J. J.; Dapprich, S.; Daniels, A. D.; Farkas, Ö.; Foresman, J. B.; Ortiz, J. V.; Cioslowski, J.; Fox, D. J. *Gaussian 09*, revision A.02; Gaussian, Inc.: Wallingford CT, 2009.

(11) (a) Steinfeld, J. I.; Francisco, J. S.; Hase, W. L. *Chemical Kinetics and Dynamics*; Prentice Hall: Upper Saddle River, NJ, 1989. (b) Eyring, H. *J. Chem. Phys.* **1934**, *3*, 107.

(12) Wolf, C. *Dynamic Stereochemistry of Chiral Compounds*; Royal Society of Chemistry: Cambridge, 2008.

(13) Fehrensen, B.; Luckhaus, D.; Quack, M. *Chem. Phys.* **2007**, *338*, 90.

(14) Neuenschwander, U.; Guignard, F.; Hermans, I. *ChemSusChem* **2010**, *3*, 75.

(15) Twigg, G. H. *Chem. Eng. Sci.* **1954**, *3*, 5.